Structural Requirements for Intramolecular Charge-Transfer in Excited State of 4-(9-Anthryl)-N,N-dimethylaniline

Aleksander Siemiarczuk

Institute of Physical Chemistry, Polish Academy of Science, Kasprzaka 44, 01-224 Warsaw, Poland

Jacek Koput

Photochemistry Group, A. Mickiewicz University, Grunwaldzka 6, 60-780 Poznan, Poland

Andrzej Pohorille

Department of Biophysics, Institute of Experimental Physics, University of Warsaw, Zwirki i Wigury 93, 02-089 Warsaw, Poland

Z. Naturforsch. **37a**, 598–606 (1982); received January 11, 1982

Excited state kinetics and other photophysical features of 4-(9-anthryl)-N,N-dimethylaniline and two model compounds have been thoroughly examined in order to establish the structural conditions for highly polar excited state formation.

Also quantum chemical calculations by means of INDO/S CI and PCILO methods have been performed to obtain potential energy curves, dipole moments and atomic charge densities for the ground and lowest excited singlet states as a function of the angle of twist between anthryl and dimethylaniline subunits.

Both the experimental and theoretical results confirm the previously proposed TICT (Twisted Intramolecular Charge-Transfer) model predicting the perpendicularity between electron donor and acceptor moieties as a condition for nearly full charge-separation in excited states for some classes of aromatic compounds.

Introduction

Formation of intramolecular charge-transfer (ICT) in excited 4-(9-anthryl)-N,N-dimethylaniline [1, 2, 3] has been previously explained in terms of the TICT model (Twisted Intramolecular Charge-Transfer Excited State) [4, 5, 6]. The model seems to be applicable to various classes of intramolecular donor-acceptor molecules (D–A) exhibiting a nearly full electron transfer from D to A in sufficiently polar solvents [6]. The TICT model predicts that in some cases, when D and A are linked together by a formally single bond, the most favourable conformation for the excited state ICT is perpendicularity of the π-electronic systems of D and A, minimizing thus their overlap. It has been shown in the case of dimethylaminobenzonitrile (DMABN) that its anomalous double luminescence could be satisfactorily explained in terms of rotation of the $N(CH_3)_2$ group in the excited state to the perpendicular conformation with respect to the benzene ring [7, 8]. It has been established that the twisted conformer of DMABN is responsible for the lower energy polar emission whereas the higher energy fluorescence arises from the untwisted precursor. Such an assignment was made after investigation of several model compounds in which the $N(CH_3)_2$ group is rotated to the planar or perpendicular conformation. In the case of anthryl derivates of dimethylaniline, I, II and III (Fig. 1), none of steric restrictions imposed did prevent the relaxation in the excited state, but they allowed at least to exclude the rotation of the $N(CH_3)_2$ group as the process leading to the polar emitting state [4]. Some indirect conclusions derived from kinetic data led

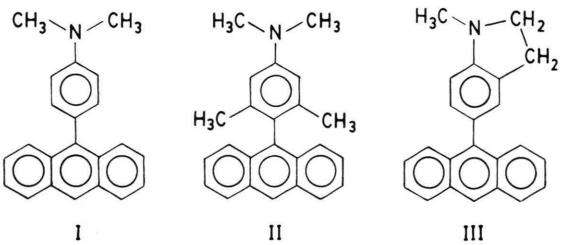

I II III

Fig. 1. 4-(9-anthryl)-N,N-dimethylaniline (I), 4-(9-anthryl)-3,5-dimethyl-N,N-dimethylaniline (II) and 1-methyl-5-(9-anthryl)-indoline (III).

Reprint requests to Dr. A. Siemiarczuk, Institute of Physical Chemistry, Polish Academy of Science, Kasprzaka 44, 01-224 Warsaw/Polen.

0340-4811 / 82 / 0600-0598 $ 01.00/0. — Please order a reprint rather than making your own copy.

us to the hypothesis of perpendicularity between anthracene and dimethylaniline (DMA) moieties in the equilibrated ICT state [4, 6]. In the meantime, Baumann proposed an alternative model based on his electrooptical measurements in absorption and emission, which have been interpreted in terms of enhanced polarizability upon excitation [9]. As he concluded, none of structural changes claimed for I, II and III in the TICT model are necessary to explain the nature of the equilibrated ICT state and the kinetics of its formation. The latter, according to Baumann, may be exclusively due to solvent reorientation around a polarizable rigid dipole represented by the excited molecule.

In order to explain the observed phenomena we present some new spectroscopic and kinetic data and results of INDO/S and PCILO calculations concerning transition energies and the ground state energy of I as a function of the angle of twist between anthryl and DMA subunits.

Materials

Syntheses of 4-(9-anthryl)-N,N-dimethylaniline (I), 4-(9-anthryl)-3,5-dimethyl-N,N-dimethylaniline (II) and 1-methyl-5-(9-anthryl)-indoline (III) were performed by Dr. A. Krówczyński and are described elsewhere [4].

The solvents were of fluorescence or spectroscopic grade. 2-methyltetrahydrofuran (MTHF) was distilled over $LiAlH_4$ before use to eliminate any contents of water.

The solutions were deaerated by freeze-pump-thaw technique.

Experimental

Steady-state fluorescence measurements were performed with a laboratory-built Jasny-type spectrofluorimeter with a regulated temperature equipment [10]. The apparatus may be used for checking of the sample transmittance at the wavelength of excitation simultaneously with emission measurements in the whole temperature range.

Fluorescence rise and decay curves were recorded with a sampling technique with nanosecond pulsed N_2 laser excitation. Fluorescence lifetimes were determined by means of a least squares method combined with a convolution of a laser pulse with an assumed fluorescence response function.

Also a dye laser pumped by N_2 laser pulses was used in order to extend the wavelength of excitation towards the red.

Results and Discussion

1. Kinetics

In the previous paper [4] a strong influence of temperature on the shape and position of the fluorescence spectra in n-butanol was reported. A rapid increase of the fluorescence bandwidth in some temperature region was attributed to the appearance of a higher energy anthracene-like emission superposing the polar one. The fluorescence band broadening could be also caused by the interactions of polar solvent molecules with excited solute molecules. This is the case when the solvent relaxation time is of the order of the fluorescence lifetime, so the molecule does not emit from the equilibrated excited state. The fluorescence spectrum is composed of many overlapping bands with slightly different transition energies reflecting different stages of solvent reorientation around excited molecules. The kinetics of the fluorescence decay is usually non-exponential and depends on the emission wavelength [12, 13].

In order to obtain better spectral resolution we measured time-resolved fluorescence spectra at the temperatures at which steady-state fluorescence broadening had been observed. These spectra are composed of two distinct bands [4, 11] indicating the existence of two emitting forms of intramolecular origin, rather than the superposition of many spectra due to stepwise reorientation of solvent molecules. The solvent relaxation probably also contributes to the band broadening, however, it is very unlikely that this process is responsible for the appearance of two distinct bands.

The interpretation has been confirmed by an examination of the rise and decay fluorescence curves detected at the short- and longwavelength edge of the fluorescence spectrum [4]. We have observed a clear correlation between the long-wavelength risetime and the short-wavelength decay-time and have proposed a model of consecutive steps leading to the ICT excited state formation:

$$\begin{array}{ccccc} X & \xrightarrow{h\nu} & X^* & \underset{\sim}{\overset{k_{xy}}{\rightarrow}} & Y^* \\ & & \downarrow k_x & & \downarrow k_y \\ & & X & & Y \end{array}, \qquad (1)$$

where X* denotes a locally excited molecule (A*–D), Y* the polar structure of the relaxed excited molecule $(A^-–D^+)^*$, k_x and k_y the total deactivation rate constants and k_{xy} the rate of intramolecular relaxation.

The lifetime of the short-wavelength local emission decreases rapidly at higher temperatures (lower viscosity). Thus in

$$1/\tau_x = k_x + k_{xy}, \tag{2}$$

$k_{xy} = k_{xy}^{\infty} \exp(-E_{xy}/RT)$ is the dominating term.

In [4] we reported the activation energy E_{xy} for II in n-butanol to be considerably lower than for the other compounds; now after additional measurements and recalculation we have obtained practically the same values for all three derivatives (Figure 2). This identity indicates that the intramolecular conversion rate is most probably controlled by the viscosity of the solvent.

Basing on the dependence of the spectral halfwidth of the fluorescence band in n-butanol on temperature (see Fig. 2 in [4]) and applying the kinetic scheme (1), one can try to estimate the rate of conversion k_{xy}. The maximal broadening of the fluorescence band is observed for compound II at 183 K. For I and III it occurs at 209 K and 203 K, respectively. Assuming that the halfwidth reaches its maximum value in the temperature interval in which both X and Y species give a comparable contribution to the total emission intensity, one gets the approximate relation

$$\frac{k_f^x}{k_f^x + k_{nr}^x + k_{xy}} \approx \frac{k_{xy} k_f^y}{(k_f^x + k_{nr}^x + k_{xy})(k_f^y + k_{nr}^y)} \tag{3}$$

and finally

$$k_{xy} \approx \frac{k_f^x}{k_f^y}(k_f^y + k_{nr}^y). \tag{4}$$

Taking appropriate values from Table 1 and from Fig. 2, the following estimations for k_{xy} are obtained:

$$k_{xy}^{I}(209\text{ K}) \approx 7 \times 10^7\ \text{s}^{-1},$$
$$k_{xy}^{II}(183\text{ K}) \approx 22 \times 10^7\ \text{s}^{-1},$$
$$k_{xy}^{III}(203\text{ K}) \approx 14 \times 10^7\ \text{s}^{-1}.$$

Assuming that the activation energies for all three derivatives are within the range of $3 \div 4$ kcal/mole, one gets the limiting values for the preexponential factor k_{xy}^{∞} presented in Table 2. These constants

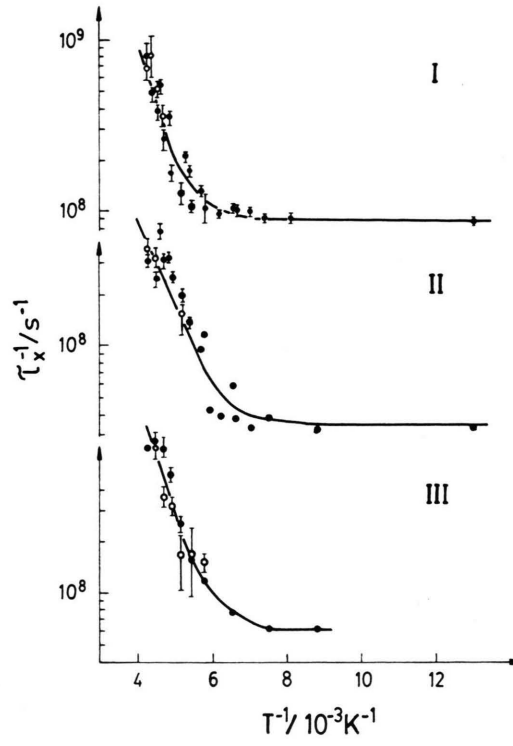

Fig. 2. Temperature dependence of the short-wave fluorescence decay-times (●) and the long-wave fluorescence rise-times (○) in n-butanol. Solid lines represent the best fit to $1/\tau_x = k_x + k_{xy}^{\infty} \exp(-E_{xy}/RT)$.

Table 1. Some photophysical parameters of I, II and III in n-butanol.

Compound	T °K	Φ_x	Φ_y	τ_x ns	τ_y ns	k_f^x 10^7 s^{-1}	k_f^y 10^7 s^{-1}	k_{nr}^x 10^7 s^{-1}	k_{nr}^y 10^7 s^{-1}
I	294	—	0.80	—	19.3	—	4.1	—	1.2
	213	—	—	—	24.6	—	—	—	—
	123	0.76	—	11.1	—	6.8	—	2.2	—
II	294	—	0.18	—	35.0	—	0.5	—	2.4
	223	—	—	—	~ 21	—	—	—	—
	113	0.66	—	29.0	—	2.3	—	1.1	—
III	290	—	0.22	—	13.6	—	1.6	—	6.0
	203	—	—	—	13.9	—	—	—	—
	113	0.53	—	17.0	—	3.1	—	2.8	—

Table 2. Estimated limiting values of absolute rates of conversion.

Compound	k_{xy}^{∞}/s^{-1}	
	$E_{xy} = 3$ kcal/mole	$E_{xy} = 4$ kcal/mole
I	10^{11}	10^{12}
II	8.4×10^{11}	13.0×10^{12}
III	2.4×10^{11}	2.8×10^{12}

fall into the range of $10^{11} \div 10^{13}$ s^{-1}, corresponding thus to typical rates of molecular vibrations. Since the preexponential factor for compound II is considerably greater than for I and III, it seems very probable that the ICT excited state corresponds to a twisted geometry of our molecules.

In order to determine the photophysical parameters of the polar excited state in terms of the kinetic model (1), the temperature effect upon fluorescence and lifetime has been thoroughly investigated. MTHF has been used as a solvent to observe pure ICT fluorescence in a wide range of temperatures. At high temperatures $k_{xy} \gg k_x$, and the quantum yield of ICT fluorescence is simply given by

$$\Phi_y = k_f^y \tau_y . \tag{5}$$

From the experimental Φ_y and τ_y values the rate constant of ICT fluorescence could be determined. As can be seen from Fig. 3, k_f^y is thermally activated for all three derivatives, and generally we can express this dependence as

$$k_f^y = k_f^0 + k_f^{\infty} \exp(-E_f^y/RT) . \tag{6}$$

Low values of k_f^0 ($< 2 \times 10^7$ s^{-1}, $< 3 \times 10^6$ s^{-1} and $< 10^7$ s^{-1} for I, II and III, respectively) indicate that the radiative process is rather strongly forbidden for the conformation at equilibrium. This is in good agreement with the TICT model, in which the perpendicularity between donor and acceptor moieties should diminish the transition moment considerably. Thermal activation of a low energy torsional vibration around the donor-acceptor bond would produce an additional transition intensity which is strongly dependent on the amplitude of the vibration. The value of the activation energy of

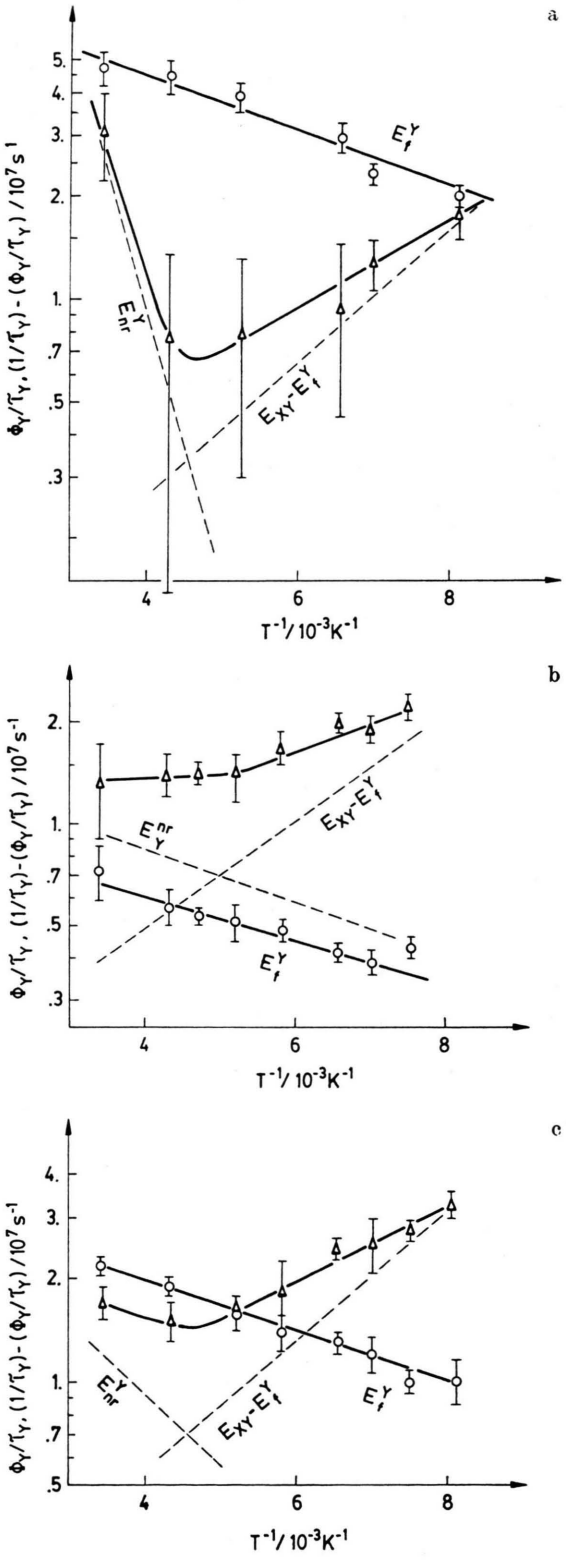

Fig. 3. Φ_y/τ_y (○) and $(1/\tau_y) - (\Phi_y/\tau_y)$ (△) versus $1/T$ for I (a), II (b) and III (c) in MTHF. Dashed lines represent the low and high temperature limit of $(1/\tau_y) - (\Phi_y/\tau_y)$.

k_f^y ($\cong 130\ cm^{-1}$) corresponds to small vibrational quanta and is consistent with the model.

The nonradiative rate constant k_{nr}^y should be expressed in the high temperature limit as

$$k_{nr}^y \cong (1/\tau_y) - \Phi_y/\tau_y . \tag{7}$$

As it can be seen from Fig. 3, the plot of the r.h.s. of (7) versus T^{-1} exhibits a minimum, indicating that the formula is not valid in the whole temperature range. By the introduction of an exact expression for Φ_y into (7), one gets

$$(1/\tau_y) - (\Phi_y/\tau_y) = k_f^y + k_{nr}^y - \frac{k_{xy} k_f^y}{k_f^x + k_{nr}^x + k_{xy}}$$
$$= \frac{(k_f^x + k_{nr}^x)(k_f^y + k_{nr}^y) + k_{xy} k_{nr}^y}{k_f^x + k_{nr}^x + k_{xy}} . \tag{8}$$

Since $k_{xy} \gg k_f^x + k_{nr}^x$ in a broad temperature range, in this approximation

$$(1/\tau_y) - (\Phi_y/\tau_y)$$
$$\cong \frac{(k_f^x + k_{nr}^x)(k_f^y + k_{nr}^y)}{k_{xy}} + k_{nr}^y . \tag{9}$$

For $k_f^y > k_{nr}^y$ (I and III), the expression (9) simplifies to

$$(1/\tau_y) - (\Phi_y/\tau_y) \cong (k_f^x + k_{nr}^x)\frac{k_f^y}{k_{xy}} + k_{nr}^y . \tag{9a}$$

If $k_f^y < k_{nr}^y$ (II), we have

$$(1/\tau_y) - (\Phi_y/\tau_y) \cong (k_f^x + k_{nr}^x)\frac{k_{nr}^y}{k_{xy}} + k_{nr}^y . \tag{9b}$$

At sufficiently high temperatures the first term in (9a) and (9b) can be neglected and the relation (7) is obeyed (left side of respective plots in Figure 3). For I and III, k_{nr}^y is markedly dependent on temperature with an activation energy E_{nr}^y of ca. 3.8 and 1.0 kcal/mole, respectively, while for II it amounts to only ca. 0.3 kcal/mole.

At lower temperatures the first term in (9a) and (9b) becomes more significant, so that $E_{xy} - E_f^y$ for I and III and $E_{xy} - E_{nr}^y$ for II can be estimated. The estimated values of E_{xy} are within $1.1 \div 1.3$ kcal/mole for all derivatives and are significantly lower than those obtained in n-butanol. Viscosity data for MTHF in our temperature range were not available, but by analogy with tetrahydrofuran and other ethers one might expect the Arrhenius factor for the MTHF viscosity to be considerably lower than that for n-butanol (for THF $E_\eta \cong 2$ kcal/mole).

2. Structural Diversity in the Ground State

The role of solvent reorientation in the kinetic behaviour has been strongly stressed by Baumann [9]. Contrary to our interpretation he claimed that an increase of polarizability upon excitation may be responsible for the highly polar structure in the excited state, and that all kinetic phenomena are explainable within the model of noncooperative solvent relaxation [12, 13]. He found that excitation at the edge of the long-wave absorption shoulder produces a strongly polar Franck-Condon (FC) state, with a dipole moment nearly equal to that of the emitting equilibrated state [6, 9].

According to Baumann, such an excitation selects the molecules strongly solvated already in their ground state, and after excitation such an oriented solvent sheath induces the redistribution of electronic charge without any accompanying changes in molecular geometry. Therefore, the question arises whether the molecules excited in such a way are really identical structurally with those emitting in the equilibrated ICT state.

The temperature dependence of the absorption spectra reported by Okada et al. [2] shows that a decrease of temperature causes strong broadening of the vibrational structure and an intensity increase of the long-wavelength tail. They interpret this effect in terms of double potential minima in the ground state, suggesting that with lowering temperature a structure favouring partial electron transfer is stabilized. Such stabilization, however, might be connected either with an intramolecular coordinate and/or with the distribution of surrounding solvent molecules.

The excitation spectra of I presented in Fig. 4 exhibit a strong temperature effect in accordance with Okada's findings. Compound III reveals a similar behaviour. The excitation spectra of II, however, are almost insensitive to temperature, except for a very slight change at the red edge of the spectrum (Figure 5).

Therefore, it seems that red-edge excitation selects molecules which are more planar in their ground state as compared to excitation at the maximum of the absorption band. The enhanced planarity causes an additional charge-transfer both in the ground and FC locally excited state, but strong charge-separation between D and A is still unfavourable in view of π-electronic delocalization

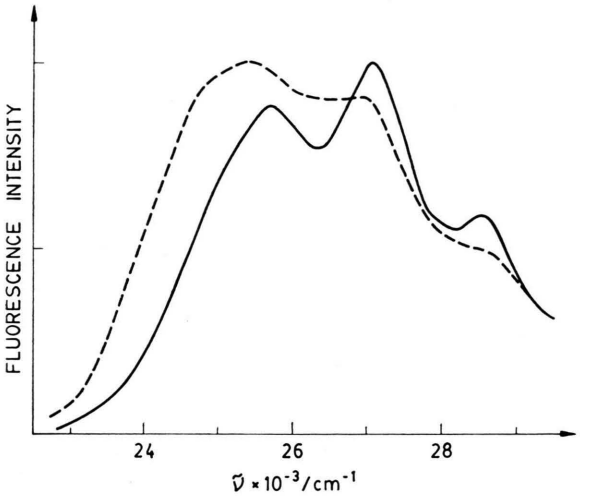

Fig. 4. Excitation spectra of I in n-butanol at 198 K (———) and at 103 K (-------).

in such a flat system. The highly polar structure [9] observed in the FC excited state for this "planar" population must be due also to strong solvation occurring already in the ground state.

To establish whether the red-edge excitation is leading directly to the ICT emitting state, we recorded decay curves of the fluorescence of I, excited at 430 nm by means of nanosecond dye-laser pulses. The estimated lifetimes in butanolic glass are ca. 8 ns when excited at 430 nm as well as at 337 nm. At a higher temperature (200 K) we observed two decays independent of the wavelength

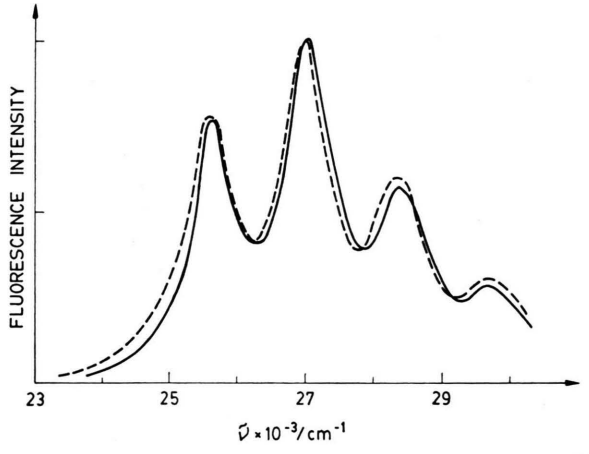

Fig. 5. Excitation spectra of II in n-butanol at 198 K (———) and at 113 K (-------).

of excitation: 6.5 ± 0.5 ns and 14.5 ± 0.5 ns corresponding to the high and low energy emission, respectively. Therefore, the "planar" conformers are not structurally identical with those responsible for ICT fluorescence.

We are dealing thus in the ground state with a distribution of conformers differing by the twist angle between anthryl and DMA. None of them is structurally identical with the molecule in the equilibrated ICT state. In such a case, the efficiency of populating of the ICT emitting state should depend on the structure of the species we are exciting. According to (1) we can describe the quantum yield of Y fluorescence as

$$\Phi_y(\tilde{\nu}_{\mathrm{exc}}) = \varphi_{xy}(\tilde{\nu}_{\mathrm{exc}})\,\theta_y\,, \tag{10}$$

where

$$\varphi_{xy}(\tilde{\nu}_{\mathrm{exc}}) = \frac{k_{xy}(\tilde{\nu}_{\mathrm{exc}})}{k_x(\tilde{\nu}_{\mathrm{exc}}) + k_{xy}(\tilde{\nu}_{\mathrm{exc}})}\,,$$

and θ_y is the intrinsic yield of Y fluorescence.

Excitation at the red-edge of the absorption band ($\tilde{\nu}_1$, "flat" conformers) and around maximum ($\tilde{\nu}_2$, more twisted forms) yields the ratio

$$\frac{\varphi_y(\tilde{\nu}_1)}{\varphi_y(\tilde{\nu}_2)} = \frac{k_{xy}(\tilde{\nu}_1)}{k_{xy}(\tilde{\nu}_2)}\,\frac{k_x(\tilde{\nu}_2) + k_{xy}(\tilde{\nu}_2)}{k_x(\tilde{\nu}_1) + k_{xy}(\tilde{\nu}_1)}\,. \tag{11}$$

At higher temperatures $k_{xy}(\tilde{\nu}_{\mathrm{exc}}) \gg k_x(\tilde{\nu}_{\mathrm{exc}})$, so that

$$\lim_{T\to\infty} \frac{\Phi_y(\tilde{\nu}_1)}{\Phi_y(\tilde{\nu}_2)} = 1\,. \tag{11a}$$

When relaxation is slowed down at lower temperatures, $k_{xy}(\tilde{\nu}_{\mathrm{exc}}) \ll k_x(\tilde{\nu}_{\mathrm{exc}})$, then

$$\lim_{T\to 0} \frac{\Phi_y(\tilde{\nu}_1)}{\Phi_y(\tilde{\nu}_2)} = \frac{k_{xy}(\tilde{\nu}_1)}{k_{xy}(\tilde{\nu}_2)}\,\frac{k_x(\tilde{\nu}_2)}{k_x(\tilde{\nu}_1)}\,.$$

Since $\tau_x(\tilde{\nu}_1) \cong \tau_x(\tilde{\nu}_2)$, therefore

$$\lim_{T\to 0} \frac{\Phi_y(\tilde{\nu}_1)}{\Phi_y(\tilde{\nu}_2)} \cong \frac{k_{xy}(\tilde{\nu}_1)}{k_{xy}(\tilde{\nu}_2)}\,. \tag{11b}$$

In Fig. 6 the ratio of the fluorescence intensity excited at $\tilde{\nu}_1 = 23000\ \mathrm{cm}^{-1}$ and $\tilde{\nu}_2 = 27000\ \mathrm{cm}^{-1}$ is plotted versus temperature. The ratio decreases monotonically with lowering temperature to the point of glass formation and then starts rising because of the overlap with emission originated from the primary excited state X*. If relation (11b) is valid, the results from Fig. 6 indicate that the rate constant of intramolecular conversion, k_{xy}, is

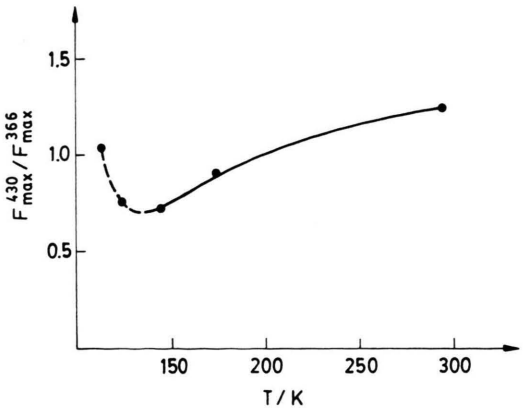

Fig. 6. Ratio of the fluorescence intensities of I excited at 430 nm and 366 nm as a function of the temperature in MTHF. Fluorescence signals have been corrected for sample absorbance and lamp intensity.

considerably lower for excitation of a more planar than a more twisted conformer. Since the intramolecular relaxation in the excited state seems to be governed by the viscosity of the solvent, the preexponential factors in the Arrhenius formula are most probably responsible for the differences in k_{xy} observed for the different conformers.

Quantum Chemical Calculations

Energies of electronic transitions, dipole moments and atomic charges as a function of the angle of twist α between the anthryl and DMA moieties were calculated by means of the INDO/S CI method described elsewhere [14, 15]. The CI procedure was performed over about 200 monoexcited configurations.

The PCILO method [16, 17] was used in addition to the INDO/S method to construct a potential energy curve as a function of α in the ground state. The INDO/S method has a spectroscopic parametrization which optimizes the electronic energy and is not appropriate for the conformational analysis where the nuclear part of the energy is essential.

In both methods, the bond lengths were taken as 1.41 for all C—C and C—N bonds and 1.1 for C—H. The bond angles were 120° in the ring as well as for C—N—C.

The distribution of the localized double bonds in the PCILO method was chosen in such a way as to minimize the calculated energy.

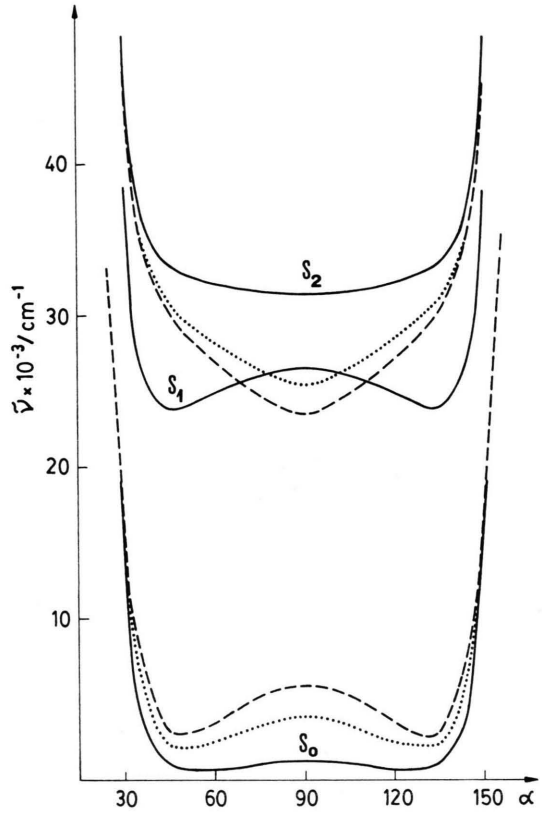

Fig. 7. Potential energy curves for the ground (S_0) and two lowest excited singlet states (S_1 and S_2) as a function of α. Dotted and dashed lines represent the potential curves after including the term (12) into S_2 and the term (13) into S_0 for ethyl ether (·····) and acetonitrile (-------) as solvents.

Excited singlet state potential curves were obtained by addition of the excitation energy to the ground state energy derived from PCILO calculations at a given value of α.

The ground state and two lowest excited state potential curves are demonstrated in Figure 7. The ^1L_b anthracene-like state has been omitted here as spectroscopically unobservable. The S_1 state, originating from the anthracene-like ^1L_a state, exhibits a moderate ICT character dependent on α (Fig. 8 and 9). Most interesting are the properties of the S_2 state, the transition to which is carrying a very small oscillator strength with a maximum value of 0.027 for $\alpha = 30°$ and vanishing at 0° and 90°. This state exhibits a very strong ICT character growing rapidly at $\alpha = 90°$. In an isolated molecule S_2 is always higher than the anthracene-like S_1 state, except for the region nearby $\alpha = 0°$, where, how-

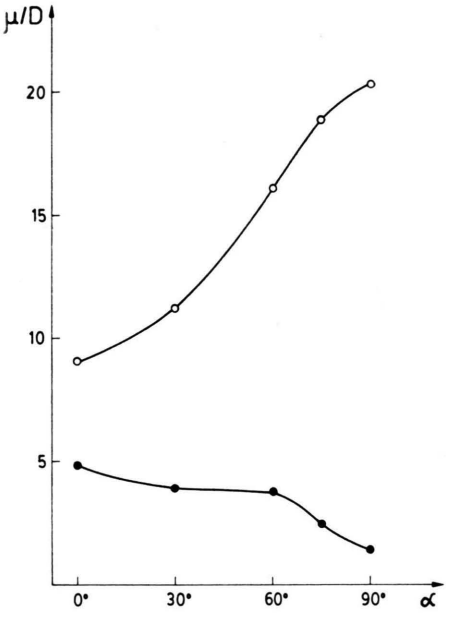

Fig. 8. Calculated dipole moments of the S_1 (●) and S_2 (○) state as a function of α.

ever, a very strong steric barrier exists. The dipole moment of S_2 calculated at 90° (20.3 D) is very close to that estimated by Okada et al. [2] (ca. 18 D) as well as to that reported by Baumann [9] (15.2 ÷ 19.3 D depending on the derivative).

Since an ICT emission has been observed only in sufficiently polar solvents, the energetic stabilization due to electrostatic interactions with solvent molecules might be reponsible for an inversion of S_1 and S_2. To check for this effect, we have applied

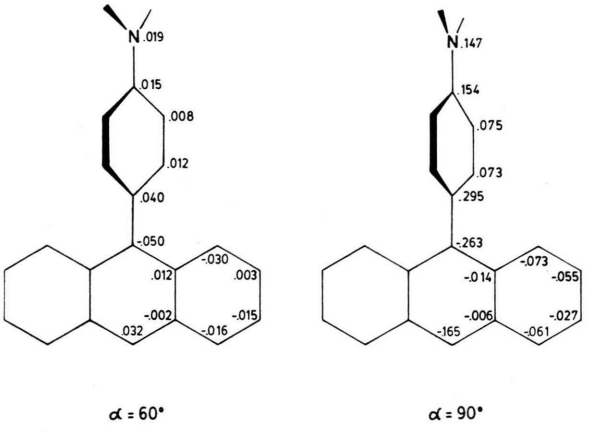

Fig. 9. Changes in net atomic charges upon excitation to S_1 at $\alpha = 60°$ and to S_2 at $\alpha = 90°$.

a classical formula based on Onsager's reaction field approximation [18, 19] in a simplified form as used by Mataga [20] neglecting the polarizability of the solute molecule:

$$E_{\text{solv}} \cong (\mu_e^2/a^3) f_\varepsilon , \tag{12}$$

where μ_e denotes the excited state dipole moment, ε the dielectric constant of the solvent, a the radius of Onsager's cavity taken after Mataga [2] as 5 Å and $f_\varepsilon = (\varepsilon - 1)/(2\varepsilon + 1)$.

As it can be seen from Fig. 7, taking E_{solv} (Eq. (12)) into consideration leads to a strong decrease of the ICT state energy, locating this state below the S_1 potential curve for the highly twisted conformation. This inversion occurs in the full range of solvent polarities where ICT emission has been observed experimentally ($\varepsilon \cong 5 \div 37$).

To compare the ICT transition frequency with experimental data, the destabilization energy of the FC ground state has been also estimated within Onsager's approximation [19, 20]:

$$E_{\text{dest}} \cong (\mu_e^2/a^3)(f_\varepsilon - f_n) , \tag{13}$$

where $f_n = (n^2 - 1)/(2n^2 + 1)$ and n is the refractive number of the solvent.

Transition frequencies have been calculated for $\alpha = 90°$ according to the TICT model and are compared with experimental ones in Table 3. Also the emission from S_1, taken simply as the transition energy at $\alpha = 45°$ from INDO/S calculations, fits very well the fluorescence transition in nonpolar solvents. Despite of an excellent agreement, it must be emphasized, however, that the Onsager radius strongly influences the calculated E_{solv} and E_{dest}. If one would apply a quantum-chemical approach [21] to calculate the solvation energy with the same radius of the cavity as we have used here,

Table 3. Calculated and experimental fluorescence transition energies of I.

Solvent	ν_{calc} cm^{-1}	$\nu_{\text{max}}^{\text{fl}}$ cm^{-1}
Acetonitrile	17,800[a]	16,700
Ethyl ether	21,800[a]	21,500
n-hexane	23,500[b]	23,600

[a] $S_2 \rightarrow S_0$ transition energy from INDO/S calculations with E_{solv} and E_{dest} included ($\alpha = 90°$).

[b] Pure $S_1 \rightarrow S_0$ transition energy calculated by INDO/S method ($\alpha = 45°$).

the obtained value of E_{solv} would be three times larger than that evaluated from the classical formula (12).

The value of $a = 5$ Å used in this paper seems to be justified since it gave a reasonable estimation of the excited state dipole moment, when the same classical Onsager's reaction field approach had been applied to the analysis of the fluorescence spectral shifts in solvents of different polarity [2].

In Fig. 9 changes in net atomic charges upon excitation to S_1 and S_2 are presented for the equilibrium conformation of the excited states ($\alpha = 60°$ for S_1 and 90° for S_2). While in S_1 there is only partial electron transfer from the DMA moiety to the anthryl one, that does not exceed 0.12 e, in the twisted S_2 state we have almost a full electronic charge flow ($\Delta q = 0.9$ e), as it has been originally predicted by the TICT model (see, for example, Fig. 5 in [6]).

The radiative transition to S_2 is forbidden because of A_2 symmetry of this state in the C_{2v} point group in planar and perpendicular conformation. In the TICT model the observed non-zero transition probability is attributed to torsional vibrations around the single bond connecting the donor and acceptor, what leads to break-up of symmetry and so gives the π-electronic coupling between both subunits. As it has been pointed out in the previous section, k_f^y exhibits an activation energy of ca. 130 cm^{-1} which is a typical value for small vibrational quanta. Approximating the potential energy curve S_2 modified by E_{solv} term nearby the minimum by a parabolic function, the harmonic frequency may be estimated as 150 cm^{-1}, being surprisingly close to the experimental value.

The results of quantum chemical calculations demonstrate the possible existence of a strongly polar ICT excited state which exhibits the features predicted by the TICT model [6]. It seems to be very unlikely, that the enhanced polarizability of the locally excited state is exclusively responsible for the ICT state formation [9]. The enhanced polarizability in the excited state may promote solvent-induced charge-separation instantaneously after light absorption, but then, the system will certainly proceed along intra- and intermolecular coordinates to reach the minimum on the potential energy hypersurface.

Acknowledgement

We are greatly indebted to Professor Zbigniew R. Grabowski for his interest and stimulating discussions.

The work was done under project 03.10.7 of the Polish Academy of Science.

[1] T. Okada, T. Fujita, M. Kubota, S. Masaki, N. Mataga, R. Ide, Y. Sakata, and S. Misumi, Chem. Phys. Letters **14**, 563 (1972).
[2] T. Okada, T. Fujita, and N. Mataga, Z. Physik. Chem NF **101**, 57 (1976).
[3] E. A. Chandross, in The Exciplex, ed. M. Gordon and W. R. Ware, Academic Press, New York 1975.
[4] A. Siemiarczuk, Z. R. Grabowski, A. Krówczyński, M. Asher, and M. Ottolenghi, Chem. Phys. Letters **51**, 315 (1977).
[5] Z. R. Grabowski, K. Rotkiewicz, and A. Siemiarczuk, J. Luminescence **18/19**, 420 (1979).
[6] Z. R. Grabowski, K. Rotkiewicz, A. Siemiarczuk, D. J. Cowley, and W. Baumann, Nouv. J. Chim. **3**, 443 (1979).
[7] K. Rotkiewicz, K. H. Grellmann, and Z. R. Grabowski, Chem. Phys. Letters **19**, 315 (1973).
[8] K. Rotkiewicz, Z. R. Grabowski, and A. Krówczyński, J. Luminescence **12/13**, 877 (1976).
[9] W. Baumann, F. Petzke, and K.-D. Loosen, Z. Naturforsch. **34a**, 1070 (1979).
[10] J. Jasny, J. Luminescence **17**, 149 (1978).
[11] A. Siemiarczuk, Ph. D. Thesis, Warsaw 1978.
[12] W. Rapp, H.-H. Klingenberg, and H. E. Lessing, Ber. Bunsen. Phys. Chem. **75**, 883 (1971).
[13] H. E. Lessing and M. Reichert, Chem. Phys. Letters **46**, 111 (1977).
[14] J. Ridley and M. Zerner, Theor. Chim. Acta **32**, 111 (1973).
[15] J. Koput, to be published.
[16] S. Diner, J. P. Malrieu, and P. Claverie, Theor. Chim. Acta **13**, 1 (1969).
[17] S. Diner, J. P. Malrieu, F. Jordan, and M. Gilbert, Theor. Chim. Acta **15**, 100 (1969).
[18] L. Onsager, J. Amer. Chem. Soc. **58**, 1483 (1936).
[19] W. Liptay, in Modern Quantum Chemistry, ed. O. Sinanoglu, Academic Press, New York 1966.
[20] N. Mataga, in The Exciplex, ed. M. Gordon, and W. R. Ware, Academic Press, New York 1975.
[21] A. T. Amos and B. L. Burrows, Adv. Quantum Chem. **7**, 289 (1973).